DOI: 10.1002/anie.201306501

Tetrel-Bonding Interaction: Rediscovered Supramolecular Force?**

*Antonio Bauzá, Tiddo J. Mooibroek, and Antonio Frontera**

Noncovalent bonding interactions are crucial in many chemical and biological phenomena and they have been intensively investigated for many years.[1] The hydrogen bond (AH···D) is probably the most studied and analyzed noncovalent interaction, where A (acceptor) can be basically any atom more electronegative than H and D (donor) can be any entity with the ability to act as an electron donor (lone pair, π system, anion, etc.).[2] Among many interactions, those involving halogen, chalcogen, and pnictogen atoms have attracted considerable attention in recent years and they are increasingly being recognized by scientists and used in supramolecular chemistry, crystal engineering, and biochemistry.[3] These interactions are moderately strong and directional because of the localization of a positive region on the extension of the covalent bonds (σ hole) in the acceptor molecule. This class of interactions has been also observed for the group IV elements. For instance, Si···N contacts have been described in the solid-state structure of $Si(ONMe_2)_4$ and related compounds by Mitzel et al.,[4,5] and Si···halide contacts have been described in perhalocyclohexasilane compounds.[6] Moreover, group IV interactions have been recently included as a subgroup of a general definition of σ-hole-bonding interactions by Politzer and co-workers.[7]

Herein we coin the term tetrel bonding for describing the tendency of heavier tetrel atoms (Tr) to interact with anions or lone-pair-possessing atoms (group IV elements are also referred to as tetrels). The binding features and structural properties of tetrel bonding are discussed, several fascinating X-ray structures are selected to illustrate the importance of this interaction, and a survey of the Cambridge Structure Database (CSD) suggests that the tetrel bonding is common in X-ray structures. The tetrel bonding is expected to be an effective and reliable instrument in crystal engineering, supramolecular chemistry, biochemistry, etc. As far as our knowledge extends, this term has not been used before to describe this interaction, which has been scarcely studied in the literature.

Recently, Taylor et al.[8] reported that the synthesis of spherosilicates is significantly improved using *n*-butylammonium fluoride (TBAF) as a catalyst. Interestingly, during the reaction work-up a new class of cage compound was obtained showing a fluoride ion perfectly centered within the octasilsesquioxane cage (see Figure 1).[9] Using NMR data the authors conclude that it essentially resembles a naked uncoordinated fluoride ion. These fluoride-encapsulated octasilsesquioxane cages can be used as small models for studying the environment that exists in zeolites. It is well known that fluoride anions act as templates in zeolite synthesis and also acts as a stabilizing agent for the zeolite building unit by electron-density transfer into the framework of silicon atoms.[10,11] This type of encapsulated compounds has been also reported for germanium-based T8 cages.[12]

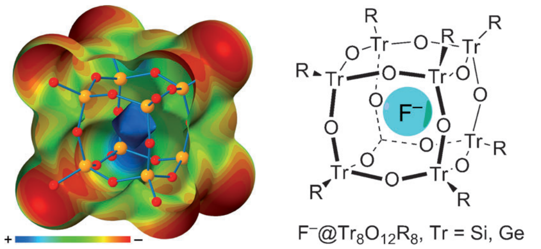

Figure 1. Right: A F^- ion encapsulated inside a $Tr_8O_{12}R_8$ cage. Left: MEPS of $SiO_{12}(OH)_8$ cage.

We have computed the interaction energies of fluoride complexes with $Tr_8O_{12}(OH)_8$ cages (Tr = Si, Ge, and Sn; see the Supporting Information for computational details). It can be observed that the binding energies are very large and negative, thus indicating a strong interaction. Consistent with related σ-hole-based interactions, the binding energy becomes more favorable toward the heavier tetrels. Since the fluoride establishes eight tetrel bonding interactions simultaneously the charge transfer is very large (> 50 % of the charge). In terms of energetic features, each individual F^-···Tr interaction ranges from 11 to 15 kcal mol^{-1}. The optimized Si and Ge complexes are shown in Figure 2 and the related X-ray structures retrieved from the CSD are also shown for comparison purposes. The energetic results gathered in Table 1 are in disagreement with experimental results, and suggests that the interaction of F^- with the Si atoms is almost negligible. This conclusion is based on the fact that fluoride ion makes very little difference to the structure. That is, the mean separation between the silicon atoms on opposite vertices of the cube is only slightly shorter in the fluoride encapsulated cage (5.306 Å) than that in the free structure (5.381 Å), and the Si···F separation in these types of fluoride cages is about 2.65 Å, which is much longer than that of a full

---

[*] A. Bauzá, Prof. A. Frontera
Departament de Química, Universitat de les Illes Balears
Crta. de Valldemossa km 7.5, 07122 Palma, Baleares (Spain)
E-mail: toni.frontera@uib.es
Dr. T. J. Mooibroek
School of Chemistry, University of Bristol
Cantock's Close, Bristol (UK)

[**] This work was funded by the MINECO of Spain (CONSOLIDER-Ingenio 2010 project CSD2010-0065, and project CTQ2011-27512, FEDER funds) and the Govern Balear (project 23/2011, FEDER funds). T.J.M. acknowledges the School of Chemistry of the University of Bristol (UK).

Supporting information for this article is available on the WWW under http://dx.doi.org/10.1002/anie.201306501.

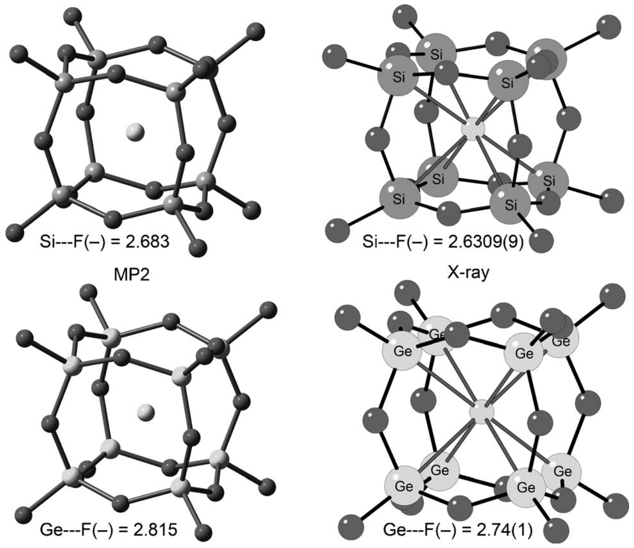

Figure 2. RI-MP2/aug-cc-pVDZ $F^-@Tr_8O_{12}(OH)_8$ optimized complexes and the equivalent X-ray structures. Distances in Å.

Table 1: Interaction energies without and with the basis set superposition error (ΔE and ΔE_{CP}, respectively), and equilibrium distances (R_e) for $F^-@Tr_8O_{12}(OH)_8$ complexes at the RI-MP2/aug-cc-pVDZ level of theory.

Complex	ΔE [kcal mol^{-1}]	ΔE_{CP} [kcal mol^{-1}]	$\Delta E_{CP}/8$ [kcal mol^{-1}]	R_e [Å]
$F^-@Si_8O_{12}(OH)_8$	−98.0	−89.3	−11.2	2.683
$F^-@Ge_8O_{12}(OH)_8$	−116.8	−108.9	−13.6	2.815
$F^-@Sn_8O_{12}(OH)_8$	−124.8	−119.1	−14.8	3.113

Si–F covalent bond (1.709 Å). This assessment is certainly true in terms of covalent bonding (the absence of any measurable Si–F coupling has been used to confirm the low degree of silicon–fluoride interaction). However, in terms of noncovalent bonding, the reported changes on the ^{29}Si and ^{19}F NMR spectra along with structural changes (the Si atoms approximate to the F^- upon binding) are in agreement with a moderately strong noncovalent interaction, as those observed in Table 1. Moreover, the molecular electrostatic potential surface (MEPS) mapped onto the van der Waals surface shows a small region of positive potential in the center of the cage (see Figure 1).

An interesting experimental finding that nicely illustrates the importance of noncovalent tetrel-bonding interactions is the formation of a crystalline chloride-bridged disiloxane.[13] The X-ray structure is shown in Figure 3 (QOMBID, top) and the bifurcated tetrel bond was defined by the original authors as a dative bond to each of the silicon centers. This is confirmed by reference to the Si-Cl distances, 2.887 and 2.731 Å, respectively, which are both substantially longer than normal covalent Si–Cl bonds (2.05 ± 0.03 Å)[13] and significantly shorter than the sum of the corresponding van der Waals radii. Furthermore, in Figure 3 (bottom) we show the X-ray structures of two binuclear pentacoordinate silicon complexes of diketopiperazine. By means of variable-temperature NMR spectroscopy and X-ray crystallography experiments the S_N2 reaction mechanism has been studied for five differently substituted analogous structures (X = F, Cl, OTf, Br, and I).[14] Two extreme cases are shown in Figure 3, wherein a covalent bond (F-Si, OYOMIZ) is observed for a very poor leaving group (F^-) and a tetrel bond (I···Si, OYOMOZ) is clearly formed for a good leaving group (I^-).

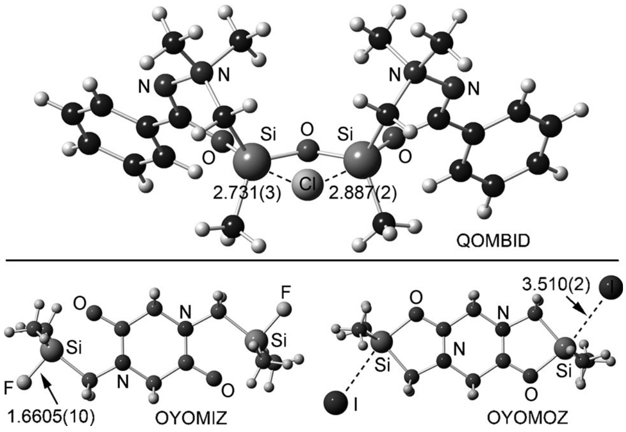

Figure 3. X-ray fragments of CSD structures QOMBID, OYOMIZ, and OYOMOZ. Distances in Å.

1, Tr = Si, X = F
2, Tr = Si, X = Cl
3, Tr = Si, X = Br
4, Tr = Ge, X = F
5, Tr = Ge, X = Cl
6, Tr = Ge, X = Br
7, Tr = Sn, X = F
8, Tr = Sn, X = Cl
9, Tr = Sn, X = Br
10, Tr = Si, Y = O
11, Tr = Si, Y = S
12, Tr = Ge, Y = O
13, Tr = Ge, Y = S
14, Tr = Sn, Y = O
15, Tr = Sn, Y = S

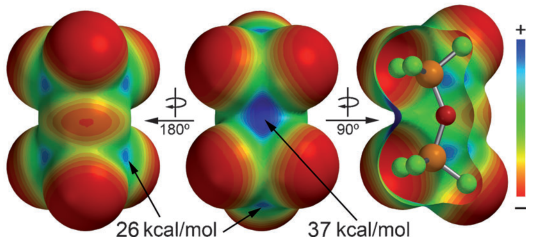

Figure 4. Top: complexes **1**–**15**. Bottom: MEPS of the F_3Tr-O-TrF_3 molecules.

We have studied computationally the tetrel-bonded complexes of perfluorodisiloxane, as a theoretical model of the experimental structure described above (QOMBID, see Figure 3), with halides. In addition we have extended our study to perfluorodigermoxane and perfluorodistannoxane to analyze the influence of the tetrel atom on the interaction strength. In addition to the anionic donors (F^-, Cl^-, and Br^-) we have also included in the study neutral donor molecules (H_2O and H_2S), as represented in Figure 4 (top). Previous to the optimization of the complexes we calculated the MEP surfaces of the F_3Tr-O-TrF_3 (Tr = Si, Ge, and Sn) molecules. The three surfaces are very similar and we have only represented the one obtained for F_3Si-O-SiF_3 in Figure 4 (bottom). The presence of four equivalent σ holes at one side of the molecule (Figure 4, bottom left) and two σ holes at both ends of the molecule (Figure 4, bottom middle) can be observed. These six σ holes are almost isoenergetic. The most positive part of the MEPS is found opposite to the four equivalent σ holes as a consequence of the superposition of two σ holes along the bisectrix of the Si-O-Si angle (obtuse part). The MEP value at this point is 37 kcal mol^{-1} for Si, 41 kcal mol^{-1} for Ge, and 45 kcal mol^{-1} for Sn. Therefore the σ hole becomes more positive toward the heavier tetrels.

The binding energies and equilibrium distances for the anionic complexes **1**–**9** are gathered in Table 2. The energies are very large in fluoride complexes because of the partial covalent bond as suggested by the very short equilibrium distances. The energetic features of complexes involving Cl$^-$ and Br$^-$ are more modest and comparable to the explanation given above for the $Tr_8O_{12}(OH)_8$ cages. As predicted by the MEPS, the energies are more favorable for the heavier tetrels and the charge transfer is very important (47–66 %). It is interesting to note the variation of the Tr-O-Tr angle, which increases upon going from fluoride to bromide and decreases upon going from Si to Sn to facilitate the simultaneous interaction with both tetrel atoms. The strong interaction energies observed for F$^-$ complexes suggest that the observation of this interaction in solution would be difficult for this anion (S_N2 reaction will likely occur), however it would be possible for the higher halides.

Table 2: Interaction energies without and with the BSSE (ΔE and ΔE_{CP}, respectively), equilibrium distances (R_e), Tr-O-Tr angle, and Merz–Kollman charges (Q_{MK}) for the complexes **1**–**9** at the RI-MP2/aug-cc-pVDZ level of theory.

Complex	ΔE [kcal mol^{-1}]	ΔE_{CP} [kcal mol^{-1}]	R_e [Å]	∡Tr-O-Tr [°]	Q_{MK} [e]
1	−89.7	−83.6	1.917	109.6	−0.43
2	−38.9	−34.0	2.497	125.0	−0.45
3	−28.9	−24.0	2.726	130.1	−0.49
4	−103.9	−96.5	1.994	108.3	−0.48
5	−57.6	−51.5	2.490	119.3	−0.40
6	−47.7	−41.7	2.662	122.3	−0.38
7	−121.0	−115.7	2.147	108.0	−0.53
8	−80.6	−75.4	2.621	117.0	−0.40
9	−72.2	−66.8	2.774	119.3	−0.34

The binding energies and equilibrium distances for the neutral complexes **10**–**15** are summarized in Table 3. The energies are obviously less favorable than those computed for the anionic complexes because of the different electrostatic nature of the donor atom. The equilibrium distances are longer, and consequently the Tr-O-Tr angle considerably increases with respect to the anionic complexes to facilitate the interaction of the lone pairs of the O/S atoms with the σ holes. The interaction energies of the water complexes are considerably more favorable than the H_2S ones and the equilibrium distances shorter, all of which is in line with the higher basicity of the oxygen atom. The geometries of some representative complexes are shown in Figure 5. In all complexes the X$^-$···Tr-F angle is close to 180°, thus indicating that the interaction is highly directional, which is similar to a halogen-bonding interaction.

Table 3: Interaction energies without and with the BSSE (ΔE and ΔE_{CP}, respectively), equilibrium distances (R_e), and Tr-O-Tr angle for the complexes **10**–**15** at the RI-MP2/aug-cc-pVDZ level of theory.

Complex	ΔE [kcal mol^{-1}]	ΔE_{CP} [kcal mol^{-1}]	R_e [Å]	∡Tr-O-Tr [°]
10	−9.3	−6.2	2.740	140.5
11	−2.8	−1.1	3.748	147.5
12	−15.2	−9.9	2.487	127.2
13	−3.3	−1.2	3.647	136.8
14	−24.3	−19.1	2.521	121.4
15	−8.3	−4.6	3.159	135.2

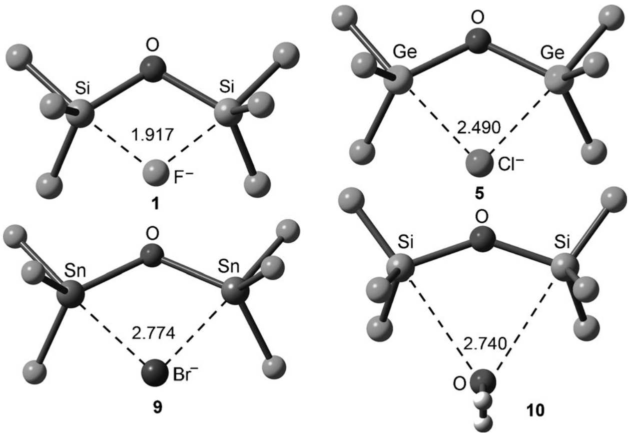

Figure 5. RI-MP2/aug-cc-pVDZ optimized geometries of some representative F_3Tr-O-TrF_3 complexes. Distances in Å.

Finally, we would like to highlight the solid-state structure of tetramethylammonium fluoride octadecasil as it has been elucidated based on powder X-ray diffraction data.[15] The topology is defined by rhombododecahedral [$4^6 6^{12}$] cages, which are linked together by hexahedral [4^6] cages, commonly referred to as double 4-rings (D4R; Figure 6). Interestingly, the octadecasil structure is acting as a ditopic carcerand, wherein the fluoride guest is confined within the D4R unit, thus forming eight tetrel bonds, and the counterion is located

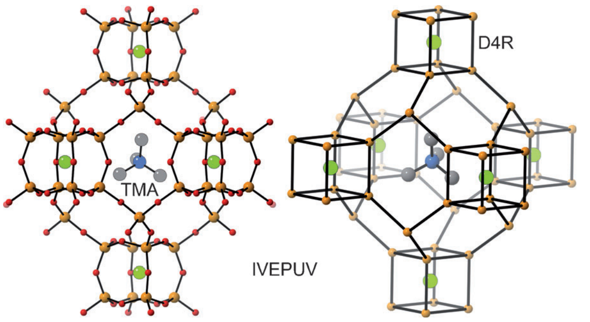

Figure 6. Partial view of the X-ray structure of TMA$^+$F$^-$-octadecasil, showing D4R units with the guest fluoride, and the [$4^6 6^{12}$] cage with tetramethylammonium ion. For clarity, the oxygen atoms have been omitted in the representation shown in the right.

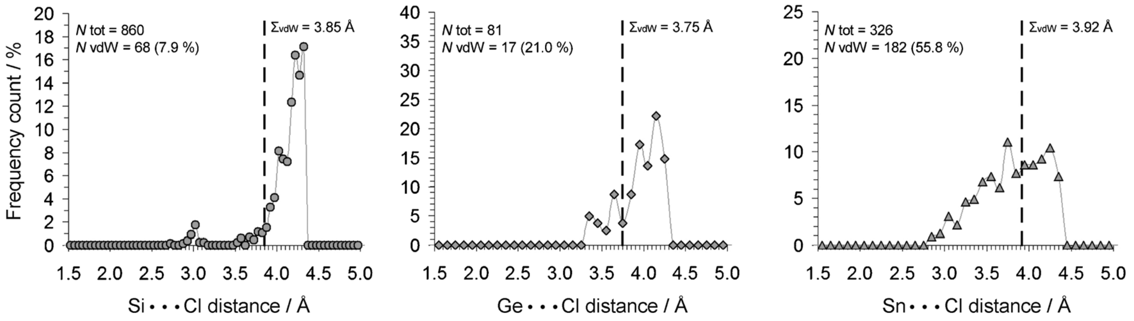

Figure 7. Plots of the frequency count [%] as a function of the $R_3Tr\cdots Cl$ distance [Å] for Tr = Si (a), Ge (b), and Sn (c). The solid lines are added as a guide to the eye and the vertical dashed lines indicate the sum of the van der Waals radii of Tr and Cl. The inset numbers represent the total amount of data (N_{tot}) and the absolute and relative mount of data displaying van der Waals overlap.

in the interior of the rhombododecahedral cages, thus forming a large number of C–H···O interactions. The oxygen atoms of the D4R units are pointing toward the exterior of the cage and concurrently toward the interior of the $[4^6 6^{12}]$ cage, thereby facilitating both tetrel-bonding interactions in the former and the hydrogen-bonding interactions in the latter.

The Cambridge Structure Database was inspected to assess whether tetrel bonding could be a generally occurring interaction within crystal structures (see the Supporting Information for details). Table 3 lists some numerical data of intermolecular distances (d) between a tetravalent tetrel atom (Tr = Si, Ge, Sn) and an electron-rich atom (El.R. = O^0, F, Cl, Br, I) where $d = \Sigma_{vdWaals+0.5}$ Å. The amount of data where overlap of van der Waals shells was observed is listed separately and, for comparison, also expressed as percentage of the total amount of data. The fraction of van der Waals overlap seems to increase on the order of Si < Ge < Sn and $O \leq F < Cl \leq Br < I$. The data for $R_4Si\cdots F$ seems to be an exception and manual inspection of the data revealed that about $^1/_3$ of the cases of van der Waals overlap are found within (engineered) cage structures such as the one shown in Figure 1.[16] As a typical example, Figure 7 shows plots of the frequency count versus the intermolecular $R_4Tr\cdots Cl$ distance (comparable plots for the rest of the data given in Table 4 can be found in the Supporting Information and reveal similar features).

Table 4: Numerical overview of data retrieved from the Cambridge Stucture Database involving tetravalent tetrel atoms and a charge-neutral oxygen or halogen atom.

	R_4Si		R_4Ge		R_4Sn	
El.R	N_{tot}[a]	N_{vdW}[b]	N_{tot}[a]	N_{vdW}[b]	N_{tot}[a]	N_{vdW}[b]
O^0	3449	118 (5.5 %)	626	177 (28 %)	678	293 (43 %)
F	1030	143 (14 %)	48	2 (4.2 %)	109	35 (32 %)
Cl	860	68 (7.9 %)	81	17 (21 %)	326	182 (56 %)
Br	151	16 (11 %)	8	3 (38 %)	45	50 (44 %)
I	102	28 (28 %)	9	4 (44 %)	25	16 (64 %)

[a] Number of data with intermolecular distances less than or equal to the sum of the van der Waals radii of Tr + El.R. [b] Number of data with intermolecular distances less than or equal to the sum of the van der Waals radii of Tr + El.R. + 0.5 Å. Value within parentheses is the percentage of the van der Waals overlap (N_{vdW}/N_{tot}) × 100.

For the distances involving $R_4Si\cdots Cl$ (Figure 7, left), the majority of the data is found to be above the $\Sigma_{vdWaals}$ benchmark, yet a small peak centered around 3 Å is observed. Such peaks are also present for the other halides as the interacting atom (not for oxygen; see the Supporting Information). These Si···Hlg data are about 0.8 Å within the sum of the van der Waals radii of the elements involved. This means that these interactions are very significant, yet not as strong as a conventional Si-Hlg bond ($\Sigma_{vdWaals}$-Si-Hlg < 1.76 Å). Such peaks were not found for $R_4Ge\cdots Cl$ (center) and $R_4Sn\cdots Cl$ (Figure 7, right), but the relative amount of overlap of van der Waals shells clearly increases on the order of Si < Ge < Sn. For $R_4Sn\cdots Cl$, more than half of the data actually is found within the $\Sigma_{vdWaals}$ benchmark (3.92 Å) and a number of short distances are found around 3 Å.

The CSD data presented above clearly suggests that noncovalent interactions with the tetravalent tetrel entities investigated are rather common within the CSD (16 % of all the data involve overlap of van der Waals shells). It must be stressed that the majority of these data are mere accidental occurrences rather than engineered. Actually, the very short (and relatively rare) Tr···El.R. distances highlighted in this paper imply that the strength of tetrel bonding can be significantly tweaked. Clearly this phenomenon presents an opportunity for (supramolecular) chemists to further explore the potential of this novel interaction.

In conclusion, we propose the use of tetrel bonding to refer to the noncovalent interaction between tetrel atoms acting as Lewis acids and any entity with the ability to act as an electron donor (lone pair, anion, etc.). Tetrel bonds have, as a minimum, comparable strength to hydrogen bonds and other σ-hole-based interactions, they are highly directional, and might serve as a new possible molecular linker. The tetrel-bonding interaction is expected to be involved in new effective and reliable instruments for crystal engineering, supramolecular chemistry, and catalysis.

Received: July 25, 2013
Revised: August 29, 2013

Keywords: ab initio calculations · group 14 elements · noncovalent interactions · silicon · supramolecular chemistry

[1] a) *Encyclopedia of Supramolecular Chemistry* (Eds.: J. L. Atwood, J. W. Steed), Marcel Dekker, New York, **2004**; b) K. Ariga, T. Kunitake in *Supramolecular Chemistry—Fundamentals and Applications*, Springer, Heidelberg, **2006**; c) *Supramolecular Chemistry: From Molecules to Nanomaterials* (Eds.: P. Gale, J. Steed), Wiley, Chichester, **2012**.

[2] E. Arunan, G. R. Desiraju, R. A. Klein, J. Sadlej, S. Scheiner, I. Alkorta, D. C. Clary, R. H. Crabtree, J. J. Dannenberg, P. Hobza, H. G. Kjaergaard, A. C. Legon, B. Mennucci, D. J. Nesbitt, *Pure Appl. Chem.* **2011**, *83*, 1619–1636.

[3] a) A. Priimagi, G. Cavallo, P. Metrangolo, G. Resnati, *Acc. Chem. Res.* **2013**, DOI: 10.1021/ar400103r; b) S. Scheiner, *Acc. Chem. Res.* **2013**, *46*, 280–288; c) S. Zahn, R. Frank, E. Hey-Hawkins, B. Kirchner, *Chem. Eur. J.* **2011**, *17*, 6034–6038.

[4] N. W. Mitzel, U. Losehand, *Angew. Chem.* **1997**, *109*, 2897–2899; *Angew. Chem. Int. Ed. Engl.* **1997**, *36*, 2807–2809.

[5] N. W. Mitzel, A. J. Blake, D. W. H. Rankin, *J. Am. Chem. Soc.* **1997**, *119*, 4143–4148.

[6] S.-B. Choi, B.-K. Kim, P. Boudjouk, D. G. Grier, *J. Am. Chem. Soc.* **2001**, *123*, 8117–8118.

[7] P. Politzer, J. S. Murray, T. Clark, *Phys. Chem. Chem. Phys.* **2013**, *15*, 11178–11189.

[8] P. G. Taylor, A. R. Bassindale, Y. El Aziz, M. Pourny, R. Stevenson, M. B. Hursthouse, S. J. Coles, *Dalton Trans.* **2012**, *41*, 2048–2059.

[9] A. R. Bassindale, M. Pourny, P. G. Taylor, M. B. Hursthouse, M. E. Light, *Angew. Chem.* **2003**, *115*, 3612–3614; *Angew. Chem. Int. Ed.* **2003**, *42*, 3488–3490.

[10] G. van de Goor, C. Freyhardt, P. Behrens, *Z. Anorg. Allg. Chem.* **1995**, *621*, 311–322.

[11] P. Caullet, J. L. Guth, J. Hazm, J. M. Lamblin, H. Gies, *Eur. J. Solid State Inorg. Chem.* **1991**, *28*, 345–361.

[12] L. A. Villaescusa, P. Lightfoot, R. E. Morris, *Chem. Commun.* **2002**, 2220–2221.

[13] I. Kalikhman, O. Girshberg, L. Lameyer, D. Stalke, D. Kost, *J. Am. Chem. Soc.* **2001**, *123*, 4709–4716.

[14] S. Muhammad, A. R. Bassindale, P. G. Taylor, L. Male, S. J. Coles, M. B. Hursthouse, *Organometallics* **2011**, *30*, 564–571.

[15] X. Yang, *Mater. Res. Bull.* **2006**, *41*, 54–66.

[16] See CSD refcodes BIDFIE, BIDFOK, CANCUR, IVEPUV, OJUYIB, WAVYAV, WAVYEZ, WAVYID, WAVYOJ, and WIJPUB.